Cyclic microindentations on monocrystalline silicon in air and in water

I Zarudi[1*], **L C Zhang**[1] and **M V Swain**[2]
[1]School of Aerospace, Mechanical and Mechatronic Engineering, The University of Sydney, Eveleigh, New South Wales, Australia
[2]Biomaterials Science Research Unit, School of Aerospace, Mechanical and Mechatronic Engineering, The University of Sydney, Eveleigh, New South Wales, Australia

Abstract: This paper studies the difference in the mechanical response of monocrystalline silicon to cyclic microindentations in air and in water. It shows that in air the indentations with a spherical indenter generated consequent phase transformations. In the first indentation cycle, the decomposition featured amorphous phase at low maximum indentation load, P_{max}, that was converged to a crystalline compound in repeated indentations. A high P_{max} generated crystalline R8/BC8 phases only. After a few cycles, the transformed material behaved linearly elastically, and its properties became stable. However, when the same indentations were conducted in water, the property stabilization process of the transformed material was significantly slowed down, featuring non-linear elasticity. It seemed that at a high P_{max} a chemical effect took place in the central part of the transformation zone.

Keywords: cyclic indentation, monocrystalline silicon, water, mechanical properties

1 INTRODUCTION

It has been shown that, in the precision machining of monocrystalline silicon, the chemical effect can play a dominant role {**1, 2**} when the machining is with water-based coolant. Thus, to control the silicon processing, the influence of water on the property changes of monocrystalline silicon is of importance.

Microindentation techniques are extremely effective in studying the mechanical properties of thin subsurface layers under different environmental conditions {**3, 4**}. On the other hand, variation in indenter shape provides the opportunity to access the effect of localized loading {**5**}. Therefore, sharp or Berkovich indenters promote shear stress and plastic contact, while blunt indenters initiate elastic contact up to the point of fracture.

Indentation of monocrystalline silicon in air has been a topic of extensive studies. It has been reported that a number of phase transformation events can take place {**6–10**}. In the first indentation cycle the diamond structure of monocrystalline silicon undergoes a phase transformation to its β-Sn structure on loading {**11, 9**}. Further transformations can be to amorphous or crystalline R8/BC8 rhombohedral/body-centred cubic phases, depending on the loading and unloading conditions {**7, 8, 11, 12**}.

Anomalous behaviour of silicon has also been observed in multiple indentations with a Berkovich indenter {**13, 14**}. Under low indentation loads the load–displacement behaviour is non-degenerative hysteresis. With increasing maximum indentation load, P_{max}, the hysteresis phenomenon disappears in the second cycle owing to crack initiation in the subsurface region.

It has been shown that silicon behaves differently when indented with a spherical indenter {**15, 16**}. The transformed structure developed in the first indentation cycle was unstable and could be altered by a number of indentation variables, such as the maximum indentation load P_{max}. It was claimed {**16**} that amorphous silicon formed in the first cycle was decomposed to crystalline R8/BC8 phase in the consecutive indentations.

A few microindentation studies have also been carried out in liquid {**3, 4, 17**}. It was shown that indentation-induced crack growth in non-metallic materials was

The MS was received on 9 May 2003 and was accepted after revision for publication on 16 December 2003.
* *Corresponding author: School of Aerospace, Mechanical and Mechatronic Engineering, The University of Sydney, Building J07, Eveleigh, NSW 2006, Australia.*

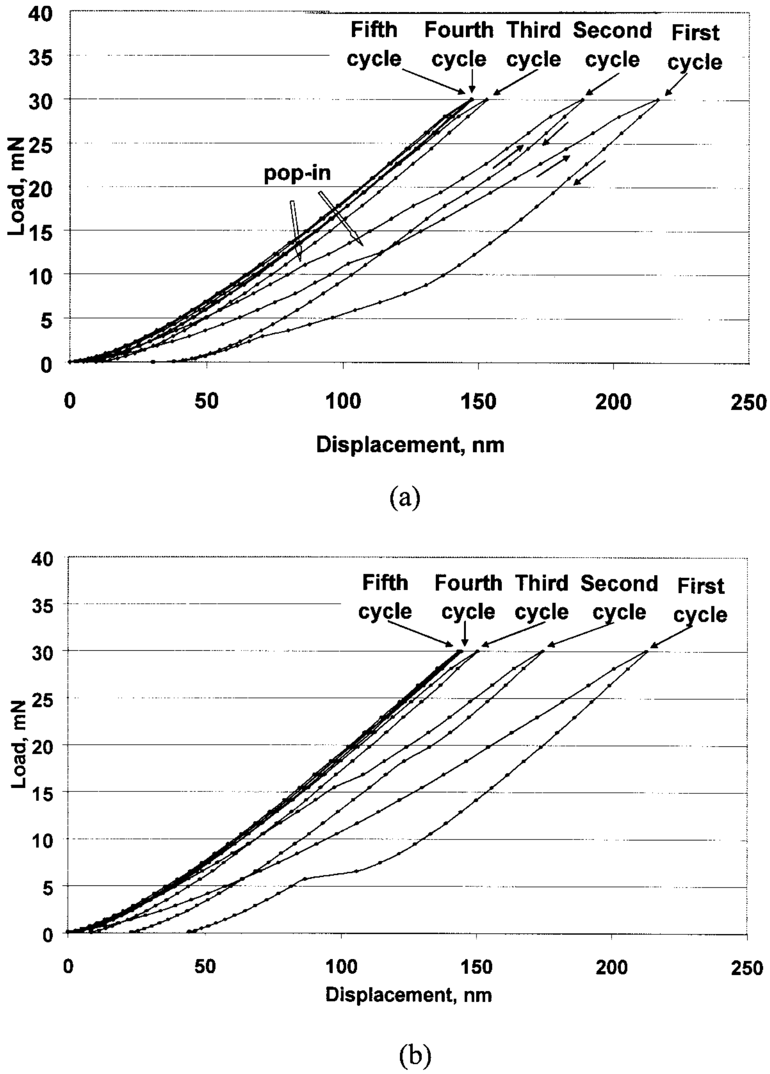

Fig. 1 Load–displacement curves in cyclic indentations with $P_{max} = 30\,mN$: (a) in air; (b) in water

more difficult in toluene than in air [17]. It was also acknowledged that the hardness of the material could be changed by environmental factors [4].

The present paper reports on the influence of water on the mechanical property changes of monocrystalline silicon and phase transformation during cyclic indentations with a spherical indenter. In all indentation experiments the maximum indentation load was kept at a sufficiently low level to exclude microcracking at the sample surface and thus to avoid water penetration in the sample subsurface.

2 EXPERIMENT

The test material was a monocrystalline silicon (100) wafer. The spherical indenter used had a nominal radius of 5 μm. The indentation tests were conducted on Ultra-Micro Indentation System-2000 (UMIS).

To capture the effect of the magnitude of the indentation load, three sets of maximum loads, $P_{max} = 30$, 50 and 90 mN, were applied. Fifty tests were performed for every P_{max}, with an average loading/unloading rate of 0.6 mN/s. To make a thermal drift correction, a holding time of 30 s was used at the maximum load.

To characterize the stress-induced structures, TEM studies were performed in a Philips CM12 transmission electron microscope, operating at 120 kV. The TEM specimens were prepared along the ⟨110⟩ cross-section [8]. At the final stage of specimen preparation, ion beam thinning was used to achieve a sufficiently thin area for TEM.

The topography of the residual indentation marks was studied by means of an atomic force microscope (AFM). The oxygen penetration in the subsurface area was determined on a scanning transmission electron microscope (STEM) VG HB601. Energy dispersive spectroscopy (EDS) was used in the indication of the chemical composition of the thin subsurface layer.

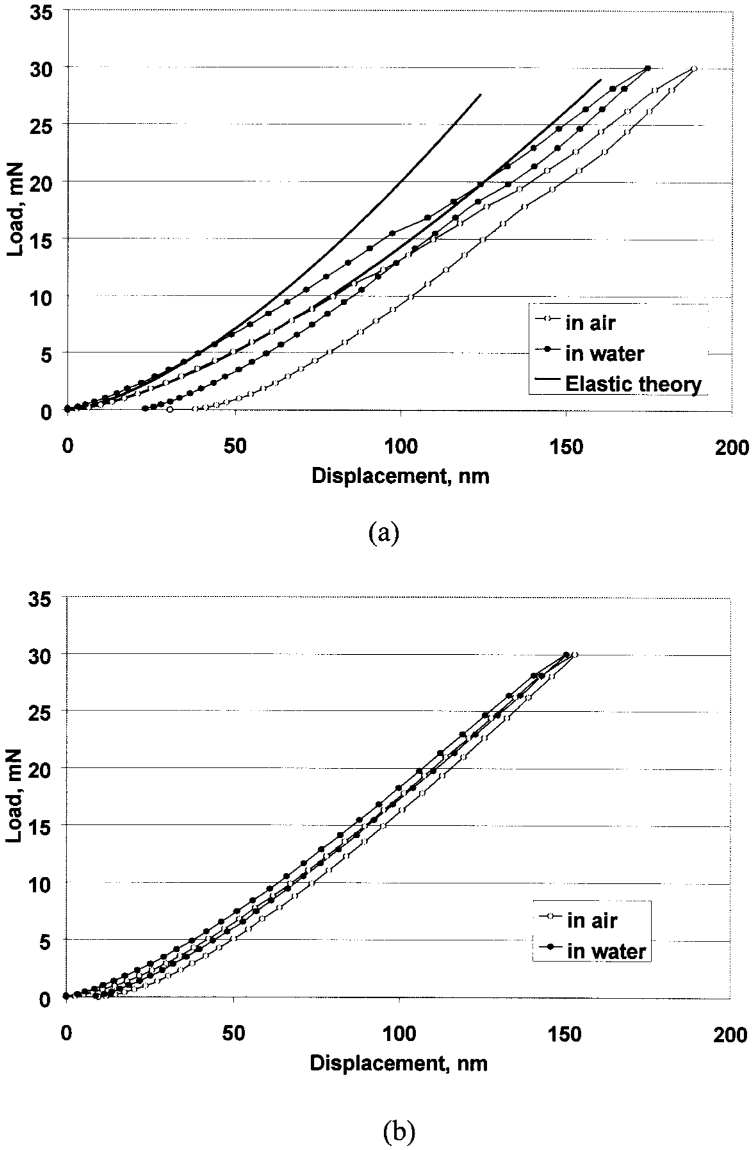

Fig. 2 Comparison of the cycles in water and air with the elastic theory ($P_{\max} = 30\,\text{mN}$): (a) second cycles; (b) third cycles

3 RESULTS AND DISCUSSION

3.1 Mechanical response of silicon in five indentation cycles

3.1.1 $P_{\max} = 30\,mN$

Figure 1 shows the progress of the load–displacement curves in the five cycles of indentations in air and water at $P_{\max} = 30\,\text{mN}$. Of the 50 indentations in air, 17 were with elbows, indicating a greater likelihood of amorphous phase transformation on unloading, and 33 were with minor pop-outs, pointing to crystalline decomposition. Out of 50 indentations in water, on the other hand, only 12 featured elbows, leaving the other 38 with pop-outs. It seems that crystalline decomposition was more likely to occur in water (76 per cent) than in air (66 per cent).

The second indentation cycle in air presents a noticeable pop-in on loading and pop-out on unloading at a much higher part of the curve when compared with that in the first indentation cycle. It was shown {**16**} that the evolution in the shape of the load–displacement curve from the first to the second cycle was due to amorphous–crystalline transformation. A comparison of the second indentation cycles in air and water (Fig. 2a) clearly demonstrates that the load–displacement curve shifted to the left much faster in water, indicating acceleration of the crystalline decomposition in the second cycle in water.

The third to fifth indentation cycles are almost identical (Fig. 2b), without hysteresis, indicating that

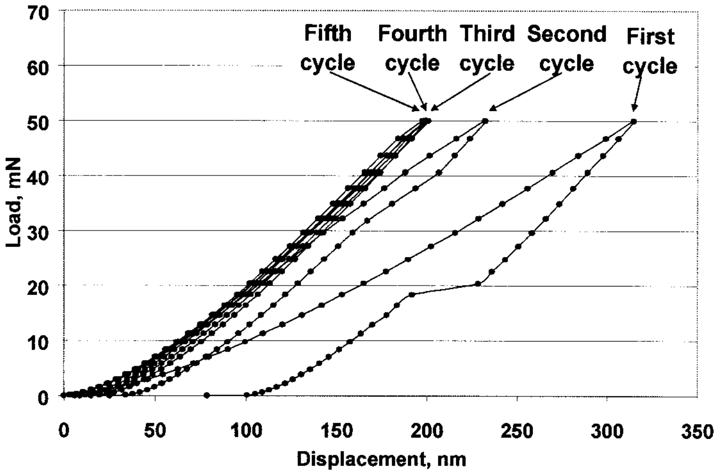

(a)

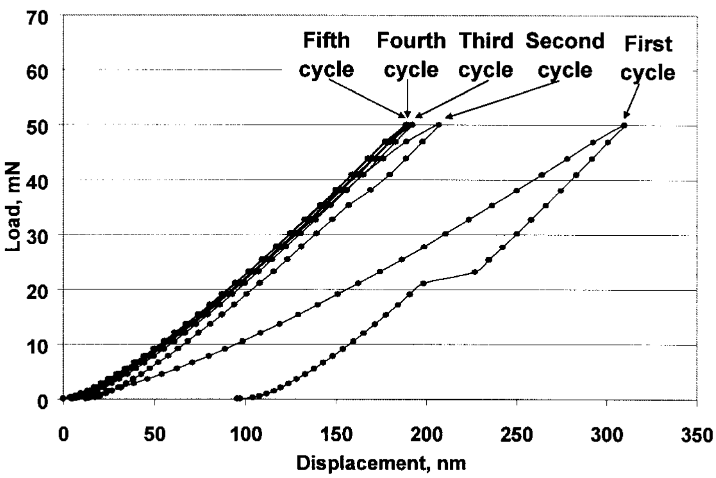

(b)

Fig. 3 Load–displacement curves in cyclic indentations with $P_{max} = 50\,mN$: (a) in air; (b) in water

the transformed materials stabilized by the cyclic indentations in air and water were similar.

3.1.2 $P_{max} = 50\,mN$

Figure 3 shows the progress of the load–displacement curves in the five cycles of indentations in air and water at $P_{max} = 50\,mN$. The pop-out appears in the first cycle, reflecting the formation of high-pressure crystalline phases in the transformation zone. In the second cycles, the slopes of the loading curves increase obviously. This is due to the penetration of the indenter into the high-pressure phases, R8 and BC8, formed in the first cycle {8}. The upper part of the curve beyond 40 mN deviates from the elastic behaviour and has a slope equal to the corresponding part in the first cycle. This seems to indicate the same type of decomposition as in the first cycle on unloading before the pop-out. The major difference between the second cycles in air and water is in their location in respect to the consecutive cycles. In air the second cycle curve deviated greatly from the third and fourth cycles, but in water the difference decreased. Similar to the case of $P_{max} = 30\,mN$, decomposition during indentations in water when $P_{max} = 50\,mN$ was also faster. Again, the load–displacement curves of the third to fifth cycles indented in water and air are very close to each other, with almost no hysteresis.

The above behaviour of silicon in the cyclic indentations is clearly different from a classical plasticity problem in which the second indentation cycle must follow the unloading path of the first cycle and after that possess non-hysteresis behaviour in the subsequent loading/unloading cycles. A close examination, as discussed below, will provide a deeper understanding of the phenomenon associated with silicon indentation.

The load–displacement responses of silicon to the indentation in air and water in the first cycle show only a

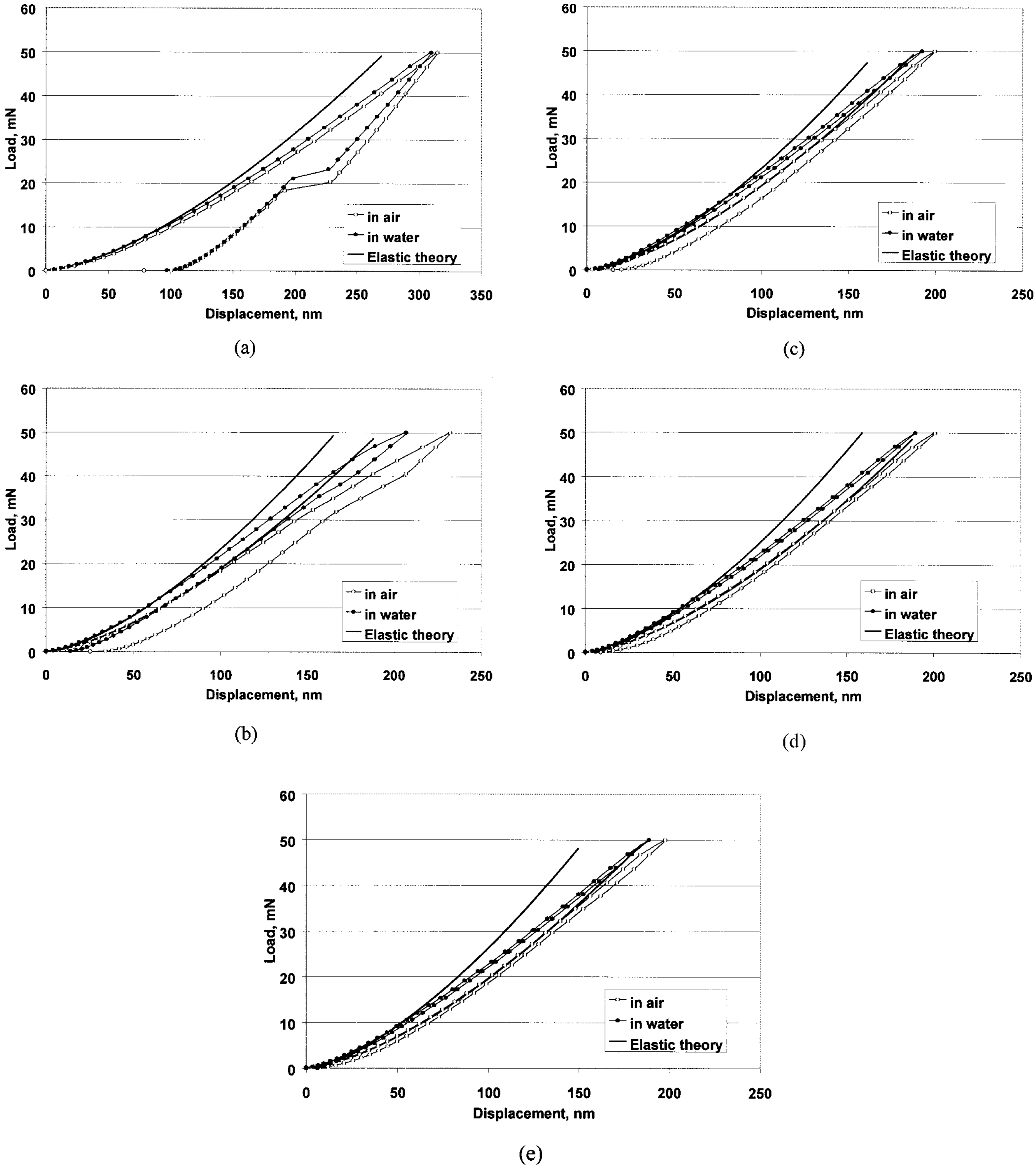

Fig. 4 Comparison of the cycles in water and air with the elastic theory ($P_{\max} = 50\,\text{mN}$): (a) first cycles; (b) second cycles; (c) third cycles; (d) fourth cycles; (e) fifth cycles

minor difference (Fig. 4a), with almost the same gradients in both the loading and unloading paths and very similar pop-out theresholds. However, the situation changes from the second cycle (Fig. 4b), in which the gradient of the loading path in water becomes higher, indicating a variation in the material properties. In the third cycle, the material behaviour in air became stable. The elastic theory gave a very good correlation with the loading part of the curve, indicating that the response of the material in air became elastic. When indenting in water, however, this did not occur. The deviation from elastic theory increased in the further indentation cycles.

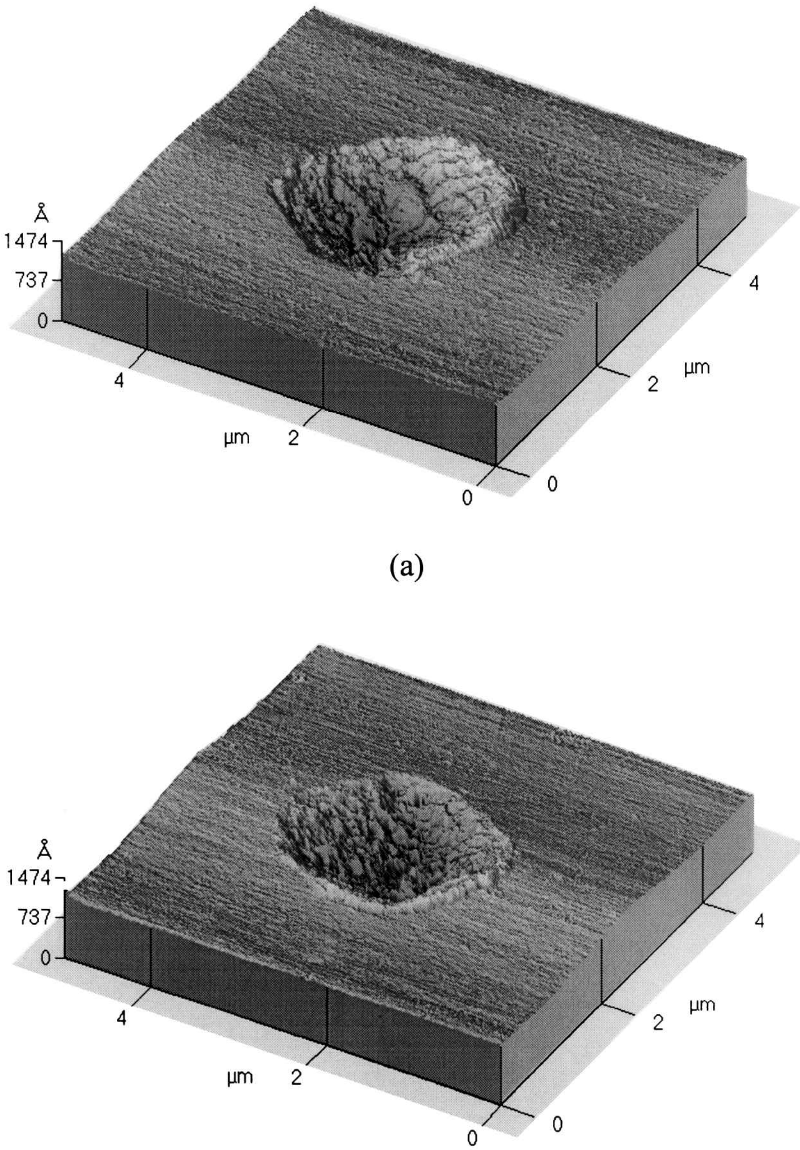

(a)

(b)

Fig. 5 Topography of the residual indentation mark after five cycles of indentations with $P_{max} = 90$ mN: (a) in air; (b) in water

Stabilization of the material was realized in cycle 4, as shown in Fig. 4e, indicating that the involvement of water slowed down the stabilization process. It was reported {**18**} that, under a greater P_{max}, the property stabilization would be even slower. This clearly concludes that the increase in P_{max} influences the property change in water.

3.2 Residual indentation marks, microstructure and oxygen distribution of the transformation zone

The residual indentation marks in air and water, as presented in Fig. 5, are clearly non-circular owing to anisotropy of silicon along different crystallographic directions {**8**}, and the indentation in air produced a greater pile-up. This seems to indicate that the ductility of the material in water decreased.

The microstructure of the transformation zone after five indentation cycles in water under different P_{max} is presented in Fig. 6. The inserts of the diffraction patterns demonstrate the crystallinity of the material. It is clear that, for all P_{max} studied, the transformation zone became crystalline after five indentation cycles. Outside the transformation zone the deformation proceeded by the extension of slip lines. At $P_{max} = 90$ mN, median and radial cracks also appeared. Compared with the corresponding structure formed by

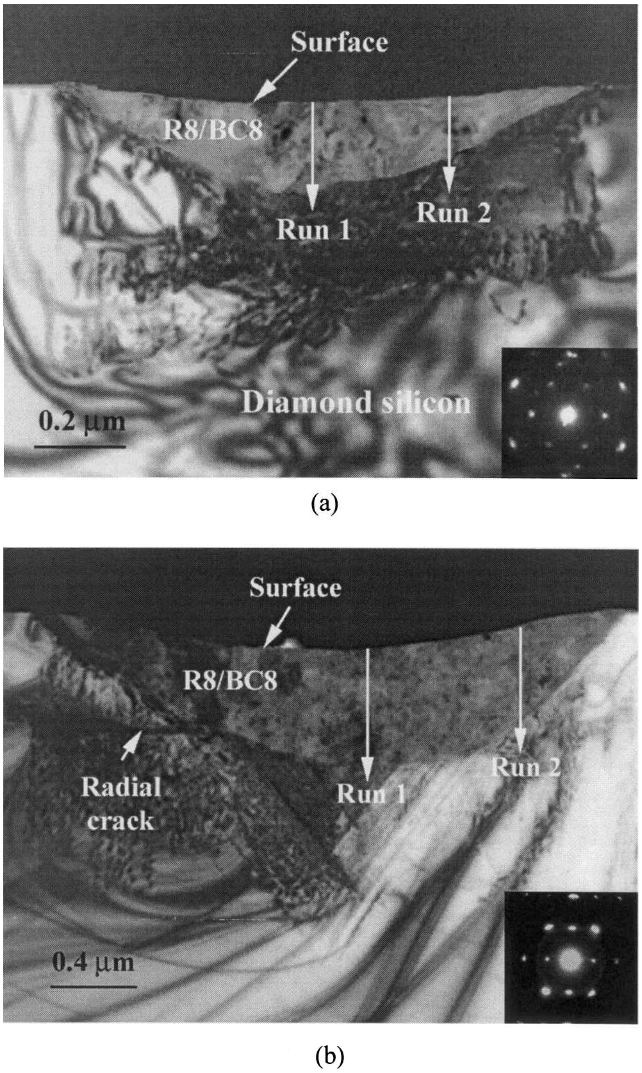

Fig. 6 Structure of the transformation zone after five indentation cycles in water: (a) $P_{max} = 30\,mN$; (b) $P_{max} = 90\,mN$

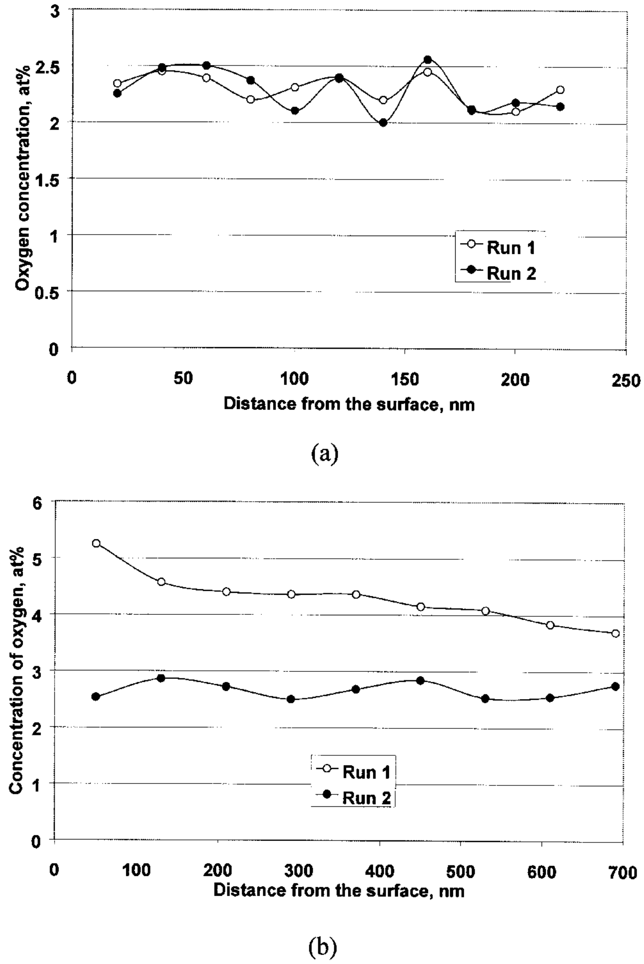

Fig. 7 Penetration of oxygen in the transformation zone: (a) $P_{max} = 30\,mN$; (b) $P_{max} = 90\,mN$

the indentations in air {**16**}, no major differences can be identified in terms of phase transformations, development of the slip lines, dislocations and microcracks.

However, the oxygen distribution in the transformation zone seems to provide some differences, as shown in Fig. 7. At $P_{max} = 30\,mN$, no additional concentration of oxygen was detected (Fig. 7a) for either run 1 or run 2 (the run locations are shown in Fig. 6). However, at $P_{max} = 50$ and 90 mN, extra concentration of oxygen was found in the central part of the transformation zone (run 1).

3.3 Discussion

The above observations identified a number of dissimilarities in the behaviour of silicon in air and water. Amorphous decomposition in the first cycle is more likely to occur in air at low P_{max}. However, in water the crystalline decomposition is accelerated, which could be due to the penetration of some elements, such as oxygen, that might increase the sites of crystal nucleation and promote the formation of crystalline phases. Amorphous–crystalline transformation was also speeded up in the consecutive indentations in water. The faster decomposition might be due to the additional nucleation sites created when indenting in water.

In air, the material in the indentation zone becomes elastic with increase in the indentation cycles. Evolution of the load–displacement curves occurs from the first to the third cycles owing to consequent phase transformations {**16**}. When the structure of the material is stabilized, it behaves linearly elastically (Figs 2 and 4).

In water, however, the elasticity turns out to be nonlinear (see Figs 2 and 4). This clearly indicates that the properties of the transformed material are influenced by the reaction with water. Since the microstructures of the materials in the transformation zones in air and water were similar (Fig. 6) but the oxygen concentration was different, it seems reasonable to conclude that, when indenting in water, the changes in the mechanical properties of the material were caused by oxygen penetration. A theoretical study using molecular dynamics analysis has confirmed the additional infringement of oxygen in the transformation zone (**19**). However, the possibility of other mechanisms could not be excluded at this stage. A further study of the atomic structure changes seems to be necessary.

4 CONCLUSIONS

By comparing the response of silicon to the cyclic microindentations in air and water, this study makes it possible to draw the following conclusions:

1. Repeated indentations in both air and water will generate consequent phase transformations. The likelihood of crystalline phase transformation during the first cycle is higher in water. Consecutive indentations accelerate amorphous–crystalline decomposition in water.
2. When silicon is indented in air, the mechanical properties of the transformed silicon will become linear elastic after a few cycles of indentations. However, when tested in water, the transformed silicon will feature a non-linear elasticity.
3. The penetration of oxygen in the central part of the transformation zone at high P_{max} seems to contribute to the changes in the mechanical properties of silicon when indented in water.

ACKNOWLEDGEMENTS

The authors wish to thank the Australian Research Council (ARC) for continuing support of this project and the Electron Microscope Unit of Sydney University for use of its facilities.

REFERENCES

1 **Zarudi, I.** and **Zhang, L. C.** Similarity and difference: damage in silicon caused by indentation, scratching, grinding and polishing. In *Abrasive Technology*, Brisbane, Australia, 1999, pp. 437–444 (World Scientific, Singapore).
2 **Zhang, L. C.** and **Zarudi, I.** Understanding of the chemical effect on the nano-wear deformation in mono-crystalline silicon components. *Wear*, 1999, **225**, 669–677.
3 **Mann, A. B.** and **Pethica, J. B.** Nanoindentation studies in a liquid environment. *Langmuir*, 1996, **12**, 4583–4586.
4 **Masuda-Jindo, K.** and **Maeda, K.** Chemical environment effect on indentation-induced fracture of silicon. *Mater. Sci. Engng*, 1994, **176**, 225–230.
5 **Bisrat, Y.** and **Roberts, S. G.** Residual stress measurement by Hertzian indentation. *Mater. Sci. Engng*, 2000, **A288**, 148–153.
6 **Weppelmann, E. R., Field, J. S.** and **Swain, M. V.** Observation, analysis, and simulation of the hysteresis of silicon using ultra-micro-indentation with spherical indenters. *J. Mater. Res.*, 1992, **8**, 830–840.
7 **Bradby, J. E., Williams, J. S., Wong-Leung, M. V., Swain, M. V.** and **Manroe, P.** Transmission electron microscopy observation of deformation microstructure under spherical indentation in silicon. *Appl. Phys. Lett.*, 2000, **77**, 3749–3751.
8 **Zarudi, I.** and **Zhang, L. C.** Structure changes in monocrystalline silicon subjected to indentation—experimental findings. *Tribology Int.*, 1999, **32**, 701–712.
9 **Clarke, D. R., Kroll, M. C., Kirchner, P. D.** and **Cook, R. F.** Amorphization and conductivity of silicon and germanium induced by indentation. *Phys. Rev. Lett.*, 1988, **60**, 2156–2159.
10 **Callagan, D. L.** and **Morris, J. C.** The extent of phase transformation in silicon hardness indentations. *J. Mater. Res.*, 1992, **7**, 1614–1617.
11 **Cheong, W. C. D.** and **Zhang, L. C.** Effect of repeated nano-indentations on the deformation in monocrystalline silicon. *Mater. Sci. Lett.*, 2000, **19**, 439–442.
12 **Domnich, V.** and **Gogotsi, Y. G.** Effect of phase transformations on the shape of the unloading curve in the nanoindentation of silicon. *Appl. Phys. Lett.*, 2000, **76**, 2214–2216.
13 **Pharr, G. M., Oliver, W. C.** and **Clarke, D. R.** Hysteresis and discontinuity in the indentation load–displacement behaviour of silicon. *Scr. Metall.*, 1989, **23**, 1949–1952.
14 **Pharr, G. M., Oliver, W. C.** and **Clarke, D. R.** The mechanical behaviour of silicon during small-scale indentation. *J. Electronic Mater.*, 1990, **19**, 881–887.
15 **Zarudi, I., Zhang, L. C.** and **Swain, M. V.** Behaviour of monocrystalline silicon under cyclic micro-indentations with spherical indenter. *Appl. Phys. Lett.*, 2003, **82**, 1027–1029.
16 **Zarudi, I., Zhang, L. C.** and **Swain, M. V.** Microstructure evolution in monocrystalline silicon during cyclic micro-indentations. *J. Mater. Res.*, 2003, **18**, 758–761.
17 **Pereira, A. S.** and **Jornada, J. A.** Environment and time dependent hardness in zirconia. *J. Mater. Res.*, 1994, **9**, 1059–1062.
18 **Zarudi, I., Zhang, L. C.** and **Swain, M. V.** Effect of water on the mechanical response of mono-crystalline silicon to repeated micro-indentations. *Key Engng Mater.*, 2003, **233–236**, 609–614.
19 **Mylvaganam, K.** and **Zhang, L. C.** Effect of oxygen penetration in silicon due to nano-indentation. *Nanotechnology*, 2002, **13**, 623–626.

